

Molecular-dynamics simulations of liquid aluminum oxide

Miguel Angel San Miguel and Javier Fernández Sanz

Departamento de Química Física, Facultad de Química, E-41012, Sevilla, Spain

Luis Javier Álvarez

Laboratorio de Simulación de Materiales, Dirección General de Servicios de Cómputo Académico, Universidad Nacional Autónoma de México, Insurgentes Sur No. 3000, Zona Cultural, Ciudad Universitaria, Coyoacán 04510, México D. F., Mexico

José Antonio Odriozola

Departamento de Química Inorgánica e Instituto de Ciencia de Materiales, Universidad de Sevilla-CSIC, E-41012 Sevilla, Spain

(Received 20 April 1998)

The total and partial radial distribution functions $g(r)$ and the corresponding structure factors $S(q)$ were calculated based on molecular-dynamics simulations in the microcanonical ensemble of liquid aluminum oxide. The simulations were performed in the temperature range 2300–3000 K in order to explore the temperature dependence of the structure, finding that the liquid structure is invariant as a function of temperature. With the aid of the partial radial distribution functions, it is possible to reinterpret the experimental data leading to a new assignment of peaks which differs from the one reported in a previously published work by Ansell *et al.* [Phys. Rev. Lett. **78**, 464 (1997)]. The structural model for liquid aluminum oxide obtained from our simulations is essentially the same as that reported in the experimental work. [S0163-1829(98)01530-6]

The determination of the structure of materials has always been subject to interpretation of experimental data. With the advent of computer simulation methods it has been possible to refine the assignment of peaks of radial distribution functions to interacting pairs of particles. Furthermore, numerical simulation allows one to avoid experimental difficulties such as having samples at extreme thermodynamic conditions. Aluminum oxide is one of the most important ceramic materials due to the great variety of technological applications.² It has a wide variety of metastable crystalline phases which are classified as α and γ series. Extensive simulation studies of the structure and dynamics of γ -alumina have been reported and the interpretation of its structure has been approached correlating simulation results with different experimental techniques.³ Recently a report of the experimental determination of the structure of liquid aluminum oxide has been published.¹ In order to complement this experiment, in this work we report the results of molecular-dynamics (MD) simulations of liquid aluminum oxide, and discuss a model to describe its structure.

The simulations were performed in the microcanonical ensemble with a system consisting of 960 particles of which 384 represented aluminum atoms and 576 oxygen atoms arranged in a cubic box. The pair interaction potential is a Pauling-type function given by

$$V_{ij}(r_{ij}) = \frac{q_i q_j}{r_{ij}} + \frac{1}{n(\theta_i + \theta_j)} \left(\frac{\theta_i + \theta_j}{r_{ij}} \right)^n,$$

where q_i are effective charges, $2.325e$ for aluminum atoms and $-1.55e$ for oxygen atoms; θ_i are the atomic radii taken from Shannon and Prewitt⁴ and n was taken to be 9 as was proposed by Adams and McDonald⁵ for ionic systems. The long-range coulombic interactions were calculated using the Ewald summation method.⁶

In order to make the simulated system comparable with the experiment reported in Ref. 1, we started with a solid corundum structure in a computational box with periodic boundary conditions, whose volume was set 20% higher than the normal to account for the volume expansion reported to occur upon melting.⁷ In order for the system to achieve the liquid disordered state, several different procedures were tested. All of them yielded the same structural rearrangements and what we report here is the result of having taken the α -alumina system into the cubic box in a first run at 300 K, in which the system just expanded to fill the computational box but there were no considerable structural changes. Then a long simulation of 100 ps at 2260 K was performed rescaling the velocities of all particles every time step. From this stage, five simulations were carried out in the temperature range 2260–2990 K. All of them consisted of a first run of 10 ps with temperature control; a second one of other 10 ps in which the system was free to evolve in order to assure the thermodynamic equilibrium; and a final one of 100 ps to calculate statistical averages. The integration of the classical equations of motion was carried out using the leap-frog algorithm with an integration time step of 1 fs. Energy fluctuations were of 0.01 kJ/mol around the mean value although there was a temperature drift in the equilibration runs of plus or minus 40 K.

Figure 1 shows the total radial distribution functions of the simulated system at 2260 and 2990 K. Figure 2 shows the structure factor $S(q)$ for the system at 2260 K obtained by Fourier transforming the corresponding $g(r)$. For the sake of comparison, the experimental results reported by Ansell *et al.*¹ have also been included in these figures. The two curves corresponding to liquid alumina in Fig. 1 are quite similar and have the same features as those for the supercooled liquid Al_2O_3 and stable liquid Al_2O_3 obtained experimentally. However, as we shall see below, the assign-

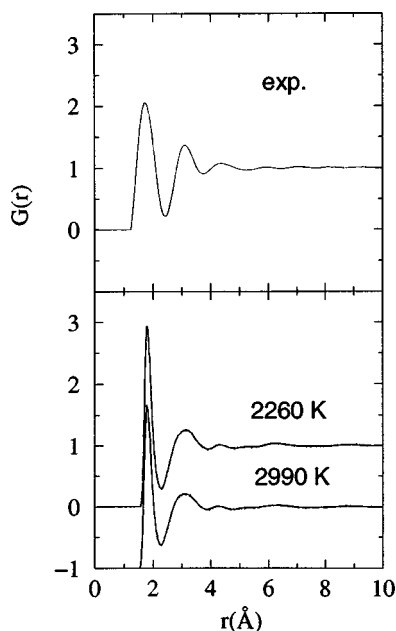


FIG. 1. Total radial distribution functions for liquid Al_2O_3 . Top: experimental spectrum at 2223 K (Ref. 1). Bottom: computed from MD simulations at 2260 and 2990 K. The values of the lower curve have been shifted by 1 for clarity.

ment of the radial distribution functions maxima differs from the interpretation reported in that work. As it can be observed both functions are in excellent agreement with the experimental data, including the fact that in the temperature range 2260–2990 K the shape of the curves is invariant as a function of temperature. The first three peaks were assigned by Ansell *et al.*¹ to the Al-O, O-O, and O-O next-nearest-

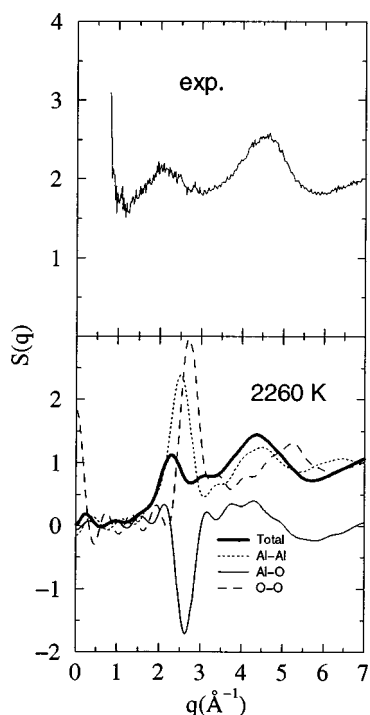


FIG. 2. Structure factor $S(q)$ for liquid Al_2O_3 . Top: experimental data at 2223 K (Ref. 1). Bottom: computed from MD simulations at 2260 K by Fourier transforming the corresponding $g(r)$.

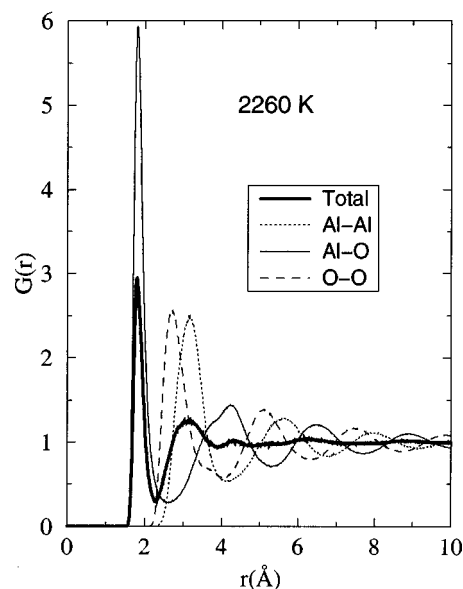


FIG. 3. Partial radial distribution functions.

neighbor pairs, respectively. However, looking at the partial radial distribution functions shown in Fig. 3, it is very easy to see the pairs which produce the main peaks of the total radial distribution function. The first peak, at 1.76 Å, is clearly due to the first coordination shell of Al, in agreement with the assignment of Ansell *et al.* The second one, at 2.9 Å in our simulations, and 3.08 Å the experimental, is a superposition of the Al-Al and O-O closest distances and not only to the O-O pair. Finally, the third peak, at 4.25 Å, is due to the second coordination shell of Al, and not to the O-O next-nearest-neighbor correlation.

The coordination number of Al atoms, obtained from the integration of the Al-O partial radial distribution functions is 4.4. This result agrees with that reported in Ref. 1 of 4.4 ± 1.0 . The ^{27}Al NMR spectrum of Al_2O_3 liquid shows a

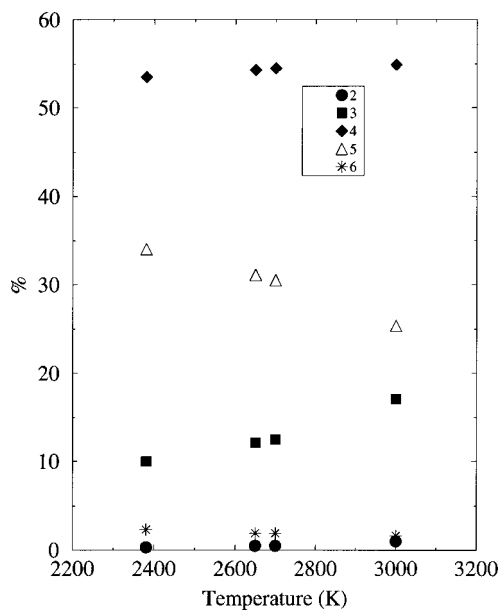


FIG. 4. Percentage of Al atoms for every coordination number at four different temperatures.

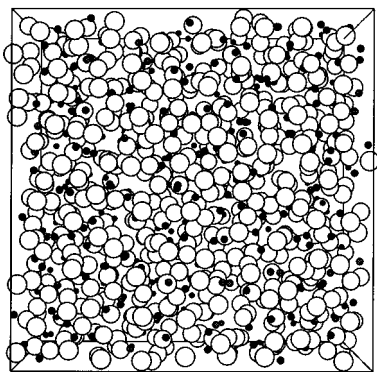


FIG. 5. Snapshot of the system in the liquid state.

single line with a chemical shift of 59 ppm.⁸ This value is between the ones corresponding to four- and six-coordinated Al sites. Coutures *et al.*⁹ originally proposed the presence of tetrahedral and octahedral aluminum atoms undergoing fast exchange and yielding an average coordination number of 4.5 atoms. Later on, Poe *et al.*¹⁰ suggested the presence of five-coordinated Al sites in the liquid. Our simulations indicate that low coordinated Al and the average coordination number is around 4.5 atoms in a wide range of temperatures.

Figure 4 presents the percentage of Al atoms for every coordination number at four different temperatures. The four-coordinated aluminum atoms are the most abundant, between 53.5 and 55 %, and increase very little with increasing temperature. The percentage of five-coordinated Al atoms diminishes with increasing temperature. This tendency is observed in the six-coordination case, whereas it is the opposite in the three-coordinated Al atoms. These are the ones which change the most with temperature at the expense of the five-coordinated Al atoms. When temperature increases, some of the five-coordinated Al go to coordination four and some of them to coordination three.

Figure 5 shows a snapshot of the system in the liquid state, from which there were extracted three pictures of representative polyhedra found in the simulated liquid, shown in Fig. 6. In the latter, the top view is a model of the most common situation and presumably the most stable in the system. This model is not stoichiometric, it has an excess of oxygen atoms, therefore the remaining Al atoms should either be low-coordinated or should form edge-sharing polyhedra as can be seen in the bottom views in Fig. 6. The bridg-

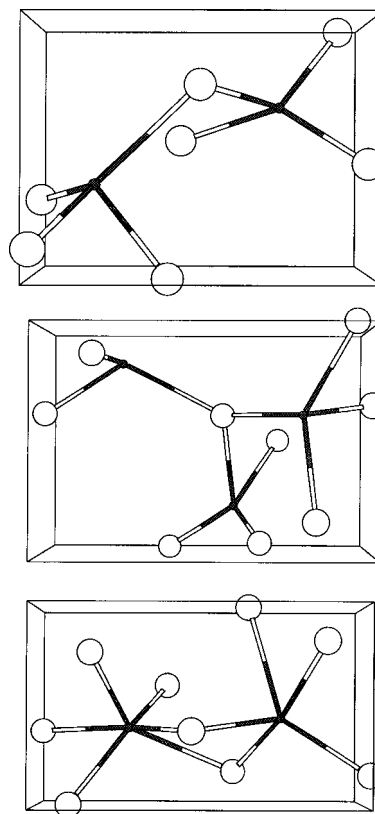


FIG. 6. Pictures of representative polyhedra found in the simulated liquid.

ing oxygen atom in the model appears as a two-coordinated atom, but in general oxygen atoms appear connected to a third low-coordination polyhedron.

Given the excellent agreement between the simulated and experimental results one can conclude that the interpretation of experimental data can be refined based on our simulations. The structural changes observed in the simulated system, including the coordination changes, are reproduced by our simulations. With the aid of the partial radial distribution functions it is possible to identify the pairs which are responsible for the peaks of the experimental total radial distribution function.

This work was supported by the DGICYT (SPAIN, Project No. PB95-1247). M.A.S. thanks the Ministerio de Educación y Ciencia for the award of a FPI grant.

¹S. Ansell, S. Krishnan, J. K. R. Weber, J. J. Felten, P. C. Nordine, M. A. Beno, D. L. Price, and M-L. Saboungi, *Phys. Rev. Lett.* **78**, 464 (1997).

²E. Dorre, *Alumina: Processing Properties and Applications* (Springer-Verlag, New York, 1984).

³L. J. Álvarez, J. Fernández Sanz, M. J. Capitán, and J. A. Odriozola, *Chem. Phys. Lett.* **192**, 463 (1992); L. J. Álvarez, L. E. León, J. Fernández Sanz, M. J. Capitán, and J. A. Odriozola, *Phys. Rev. B* **50**, 2561 (1994); *J. Phys. Chem.* **99**, 17 872 (1995); L. J. Álvarez, A. L. Blumenfeld, and J. J. Fripiat, *J. Chem. Phys.* (to be published).

⁴R. D. Shannon and C. T. Prewitt, *Acta Crystallogr., Sect. B:*

Struct. Crystallogr. Cryst. Chem. **25**, 925 (1969).

⁵D. J. Adams and I. R. McDonald, *Physica B* **79**, 159 (1970).

⁶P. P. Ewald, *Ann. Phys. (Leipzig)* **64**, 253 (1921).

⁷P. Tyrolerova and W. K. Lu, *J. Am. Chem. Soc.* **52**, 77 (1969).

⁸R. K. Sato, P. F. McMillan, P. Dennison, and R. Dupree, *J. Phys. Chem.* **95**, 4483 (1991).

⁹J-P. Coutures, D. Massiot, C. Bessada, P. Echegut, J-C. Rifflet, and F. Taulelle, *C. R. Acad. Sci., Ser. II: Mec., Phys., Chim., Sci. Terre Univers.* **310**, 1041 (1990).

¹⁰B. T. Poe, P. F. McMillan, B. Cote, D. Massiot, and J-P. Coutures, *J. Phys. Chem.* **96**, 8220 (1992).